STRONTIUM DOPING EFFECT ON ELECTRICAL, STRUCTURAL, MICROSTRUCTURAL AND MAGNETO-TRANSPORT PROPERTIES IN COLOSSAL MAGNETORESISTIVE $La_{0.7}Ca_{0.3-X}Sr_XMnO_3$ (X = 0, 0.02,0.04,0.06, 0.08,0.10) AT SINTERING TEMPERATURE OF 1220°C

[1]R.Ramli, [1]L.S. Ewe, [1]Mastura Johar

[1]College of Engineering, Universiti Tenaga Nasional, Km 7, Jalan Kajang-Puchong, 43009 Kajang, Selangor, Malaysia

For Correspondence; Rogemah@uniten.edu.my

***ABSTRACT*:** *In this research the Strontium doping effects for the magneto-transport and electrical properties under the colossal magnetoresistive $La0.7Ca0_{.3-x}Sr_xMnO_3$ (x = 0, 0.02, 0.04, 0.06, 0.08, 0.10) at sintering temperatures of 1220 ◌C have been studied. For the preparation of the material co-precipitation method were used. From the XRD patterns it is exposed that the samples have an orthorhombic structure and the diffraction patterns can be indexed with the Pbnm space group. The insulator metal transition, (T_{IM}) increased with increasing strontium doping concentration. The magneto resistance (MR) measurements were made in magnetic fields from 0.1 to 1.0 T at room temperature. The percentage of MR is increased with the increasing of magnetic field and strontium doping concentration. Variable range hopping and small polaron hopping models were used to compute the density of states at the Fermi level $N(_{EF})$ and the activation energy level (E_a) of the electron. Strontium doping concentration of x = 0.06 for sintering temperature of 1220 °C showed the highest value (~ 18.57 %) of MR at 1.0 T magnetic field.*

1. INTRODUCTION

The mixed-valence manganese perovskite $Re_{1-x}A_xMnO_3$ (where Re=La,Pr,Nd etc., and A=Ca, Sr, Ba etc.) have recently attracted considerable attention because of a huge negative magnetoresistance (Colossal Magnetoresistance, CMR) near the curie temperature, interesting structural, electrical and magnetic properties [1, 2, 3]. These exotic properties have been thought to be the result of interplay between the electron –phonon and exchange interaction [4, 5]. The characteristic and magnetic effects of these materials were explained by Zener et al. [6,7] through double exchange (DE) mechanism. Mn presents in two oxidation states Mn^{4+} and $Mn3^{+}$ and the compound is in the mixed state of $A^{3+}{}_{1-x}B^{2+}{}_xMn^{3+}{}_{1-x}Mn^{4+}{}_xO^{2-}$ [8]. The ratio of Mn^{3+}/Mn^{4+} have to be equal to the A^{3+}/B^{2+} for charge neutrality. The extreme compounds x=0 and x=1 are not mix valence. Therefore, doping with B equivalent can change the valence of the Mn ions from +3 to +4 [8].

According to Hund's rules, in order to minimize the energy, all the unpaired electron in the outer d-sell have their spin parallel to one another. Without holes doping, parent compound such as $LaMnO_3$, $PrMnO_3$ and $NdMnO_3$ are insulator at all temperatures. The manganites doped with calcium and strontium received much attention due to the high *Tc* and small varience of the B site ionic radii [9,10,11,12]. $La_{1-x}Ca_xMnO_3$ is among the most studied compound of the manganite family. The reasons for its popularity are its robust magnetoresistance effect, larger than in other much-studied material such as $La_{1-x}Sr_xMnO_3$. $La_{1-x}Ca_xMnO_3$ is usually labelled as a "low" bandwidth manganite, but it may be better to consider it as a representative of "intermediate" bandwidth compounds. The reason is that this material still has a ferromagnetic metallic phase and is only induced by external magnetic fields. The phase diagram of this series was first described by Jonker et al. [3] and recently revised by Troyanchuk *et al*. [13] and Schiffer *et al* [14]. $La_{1-x}Ca_xMnO_3$ who first studied in the full range of densities $0 < x < 1$ by Schiffer *et al*. [14]. For x=0, every Mn ion in the system suffers a static Jahn-Teller distortion and an ascribed orbital ordering such a way the ferromagnetic planes antiferromagnatically coupled arise. For x = 1, only Mn^{4+} is possible and the conduction band is empty and produce a material that behave antiferromagnetic insulator with G-type antiferromagnetism, but this time there are no Jahn-Teller distortions at all and the antiferromagnetic superexchange among t_{2g} levels domains the magnetic ground state. For intermediate values of x, Mn^{3+} and Mn^{4+} are present and metallic behavior is possible [3]. The special Ca concentrations (x) in $La_{1-x}Ca_xMnO_3$ is x = N/8 with N = 1, 3, 4, 5, 7. T_c becomes maximum at x = 3/8 and T_{co} peaks at x = 5/8. The system at x = 1/8 concentration, also, undergoes two transition which is ferromagnetic transition and antiferromagnetic transition [13, 14, 3].

Dagotta *et.al* [15] reported the behavior of $La_{1-x}Sr_xMnO_3$ with doping concentration $0 < x < 0.6$. For doping concentration ~ $0.16 < x < 0.49$, this material is ferromagnetic metal (FMM) at $T < T_c$ and paramagnetic insulator (PMI) at $T > T_c$. At $x <$ ~ 0.16, a canted spin antiferromagnetic insulating state (CSI) or a ferromagnetic insulating state (FMI) is often encountered. Usuallycharge ordering can occur in this range. High T_c (~ 370 K) was observed at doping concentration of x = 0.33 and there are two phases that occur in this concentration which is ferromagnetic phase and paramagnetic phase. The region above T_c is semiconductor, unexpected characteristic can occur when paramagnetic region is changed to metal when temperature is decreased [15,16]. In view of these results, it is interesting to study the effect of strontium doping in B sites on the electrical, structural, microstructural and magneto-transport properties of LCSMO.

2. MATERIAL AND METHODS

The bulk samples of $La_{0.7}Ca_{0.3-x}Sr_xMnO_3$ (x = 0, 0.02, 0.04, 0.06, 0.08 and 0.1) were prepared by using co-precipitation (COP) method. Lanthanum acetate, calcium acetate, strontium acetate and manganese acetate with purity ≥ 99.9 % were weighed and dissolved in glacial acetate acid. 0.5 M oxalic acid was added to the solution in an ice bath and a uniform, stable, white suspension was ammased. The resulting slurry was filtered after 5 minutes of reaction and dried in oven at 80 ^oC for 8 hours. The powders are then

calcined at 900 °C in air for 12 hours to produce in the end a black powder which was then cooled to room temperature at 2 °C/min. The calcined powders was regrounded and pressed into pellets of ~12.5 mm diameter and 2 mm thickness and then the pellets was sintered at sintering temperature 1220 ˚C for 24 hours and slowly cooled to room temperature at 2 °C /min. The phase purity of the sample were examined by using X-ray diffraction (XRD) and the surface morphology was analyzed by a scanning electron microscope (SEM). Next, magnetoresistance (MR) measurement was carried out in the present of magnetic field from 0.1 T until 1 T at room temperature. Finally, the temperature dependence of resistivity was studied in temperature range of 50 K – 300 K in zero field using the standard four-probe method. From SEM image, grain size and porosity of the sample can be calculated. The grains size were calculated by using intercept method while porosity of the sample were calculate using the equation porosity = $\frac{\rho_{theory}-\rho_{exp}}{\rho_{theory}} \times 100\%$. while theoretical density(ρ_{theory}) and experimental density(ρ_{exp}) are calculated by $\rho_{theory} = \frac{JMR}{V_{abc}}$ and $\rho_{exp} = \frac{mass}{\pi tr^2}$, respectively.

3. RESULTS AND DISCUSSION

The X-ray diffraction patterns (Fig. 1) showed that all the samples are single phase with orthorhombic structure (space group: *Pbnm*). With the increase of *x*, the intensities of the diffraction peak are slightly changed and there are no peak shifting observed for all the samples. From Fig.1, it is seen that no impurities was indicated. Jin et al. found that LCSMO (x = 0) is the single phase with the rhombohedral structure but, the sample of the LCSMO (x = $\frac{1}{3}$) has two phases (one is the rhombohedral phase and the other is the pseudo-cubic phase) and the main phase has the rhombohedral structure [17].

The lattice parameter and unit cell volumes obtained for different Sr-doping are shown in Table 1. It is seen that the cell volumes are found to increase continuously with increasing strontium concentration except for *x* = 0.10. It is may be attributed to the fact that an ion (Ca^{2+}) with smaller ionic radius (0.99 Å) is replaced by an ion (Sr^{2+}) of larger ionic radius (1.12 Å) [18].

Table 1 Lattice parameter and unit cell volume of $La_{0.7}Ca_{0.3-x}Sr_xMnO_3$

Sr Doping	a	Lattice parameter (Å) b	c	Cell volume (Å)
x = 0	5.442	7.623	5.485	227.54
x =0.02	5.477	7.770	5.458	232.27
x =0.04	5.489	7.731	5.494	232.50
x =0.06	5.480	7.750	5.482	232.82
x =0.08	5.466	7.745	5.512	233.35
x =0.10	5.480	7.726	5.473	231.72

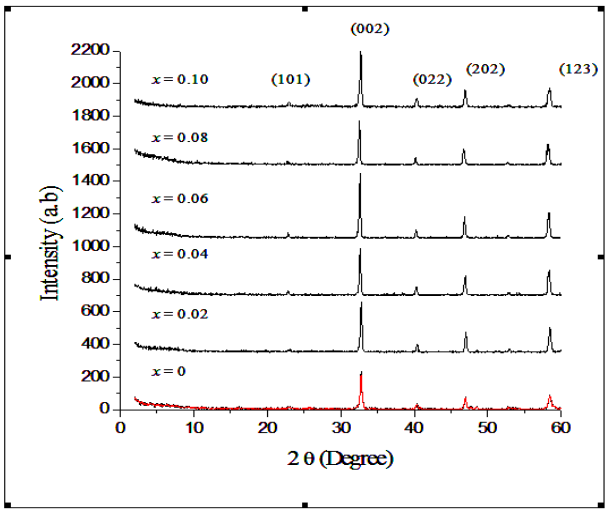

Figure 1 X-Ray diffraction pattern of $La_{0.7}Ca_{0.3-x}Sr_xMnO_3$

The variation of resistivity as a function of temperature (ρ –*T*) for all samples in the temperature range 50-295 K is shown in Fig. 2. In pure $La_{0.7}Ca_{0.3}MnO_3$ (*x* = 0), an insulator-metal transition temperature (T_{IM}) was observed at ~247 K. The T_{IM} shift successively towards higher temperature with the increase of strontium concentration until *x* = 0.08 as shown in Table 2. For *x* = 0.10, the T_{IM} value was observed at ~289 K. Jeong et al. and Im et al. have found the T_{IM} for $La_{0.7}Ca_{0.3}MnO_3$ that prepared by conventional solid state reaction is around 240.5 K and 240 K [19,20]. Furthermore, Ewe at al. has also reported that T_{IM} for $La_{0.7}Ca_{0.33}MnO_3$ prepared by COP method is around 272 K [21].

T_{IM} values were very dependent on the diffusion process that controls the growth of the grain [22]. The decrease in grain size increased the magnetically disordered states on the surface of the grains therefore double exchange (DE) mechanism was weakened and resistivity was enhanced [23]. Here, the shift of T_{IM} towards higher temperature region can be explained as the enhancement of grain growth that improved the connectivity between the grains and reduced the existing of the pores and voids as shown in Table 2.

Table 2 Grain size, T_{IM}, density and porosity of $La_{0.7}Ca_{0.3-x}Sr_xMnO_3$

Sr Doping	Grains size (μm)	T_{im} (K)	Density (ρ_{exp}) (g/cm^3)	Porosity (%)
***x* = 0**	33.4	247	5.74	6.79
***x* = 0.02**	33.6	264	5.72	7.26
***x* = 0.04**	42.8	290	6.05	2.07
***x* = 0.06**	45.6	284	6.09	1.28
***x* = 0.08**	39.8	291	5.68	7.98
***x* = 0.10**	30.5	289	5.53	10.45

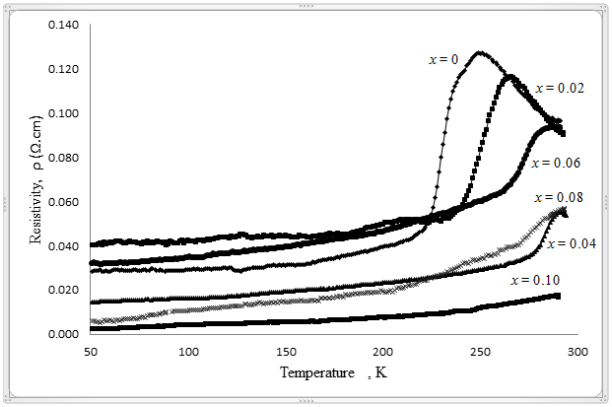

Figure 2 Resistivity versus temperature curve for $La_{0.7}Ca_{0.3-x}Sr_xMnO_3$

The surface morphology of $La_{0.7}Ca_{0.3-x}Sr_xMnO_3$ (x = 0, 0.02, 0.04, 0.06, 0.08, 0.10) compounds was analyzed by SEM and the result are presented in Fig. 3. When the grain size increased, the grain becomes more densely packed resulting in narrowing of the grain boundary regions since higher sintering temperatures (1220 ^{0}C) are expected to yield larger crystallite sizes that has reduced the strain as compared to smaller grain size. The same results have been reported in $La_{0.7}Ca_{0.3}MnO_3$ synthesized at 500, 600, 900 and 1300 ^{0}C [24].

The sample with x = 0.10 is well separated by smaller grains and the grains do not seem to connect tightly. While for doping concentration of x = 0.04 and x = 0.06 possesses well-formed granular crystallite with larger grain size. The effect of grain size on charge-ordering and phase segregation of $Nd_{0.5}A_{0.5}MnO_3$ (A= Ca & Sr) showed that sample with smaller grain size sintered at 1173 K has greater feromagnetic (FM) interaction at lower temperature due to phase segregation, compared to the sample with the largest grain size sintered at 1673 K [25].

Fig. 4 shows the magnetoresistance versus magnetic field curve of $La_{0.7}Ca_{0.3-x}Sr_xMnO_3$ (x = 0, 0.02, 0.04, 0.06, 0.08, 0.10). The percentage of MR of all the samples has been computed at room temperature by using $MR = \left(\rho_{(o)} - \frac{\rho_{(H)}}{\rho_{(o)}}\right) \times 100\ \%$, where $\rho_{(o)}$ and $\rho_{(H)}$ are the electrical resistivity at a given temperature in the absence and presence of a magnetic field, respectively. With the increasing magnetic field from 0.1 T to 1.0 T, MR (%) was found to increase and can be attributed to the suppression of spin fluctuations when the spins are aligned. Furthermore, with the increase of strontium doping, the value of MR begin to decrease firstly and then increase until the maximum value of MR (~18.75) appeared at x = 0.06. MR value are found to decrease when doping concentration increase from x = 0.08 to x = 0.10. It is well known that the smaller the grain size, the more grain boundaries there are in the sample. Research from Jin et al. found that the smallest grain size shows a maximum value of MR at 77 K [26].

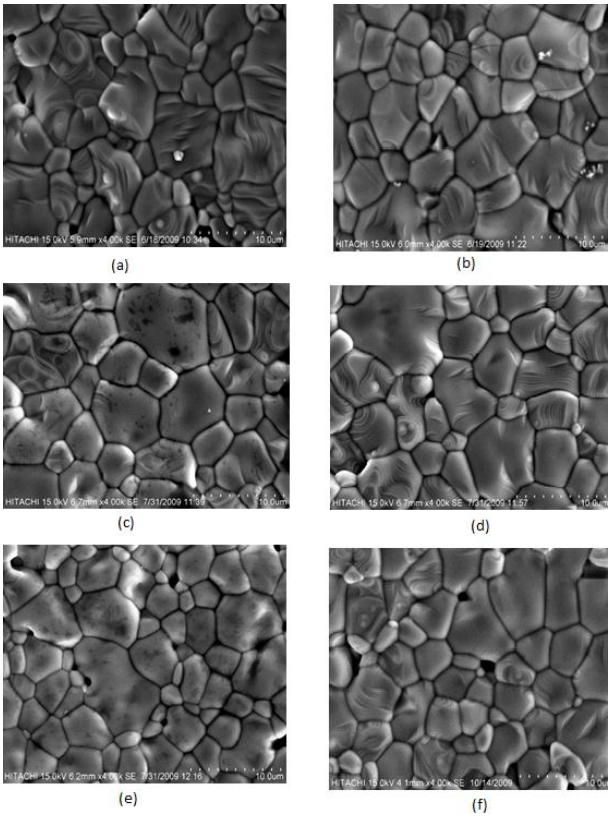

Figure 3 SEM micrograph of internal section of $La_{0.7}Ca_{0.3-x}Sr_xMnO_3$, (a) x = 0, (b) x = 0.02, (c) x = 00.4, (d) x = 0.06, (e) x = 0.08 and (f) x = 0.10

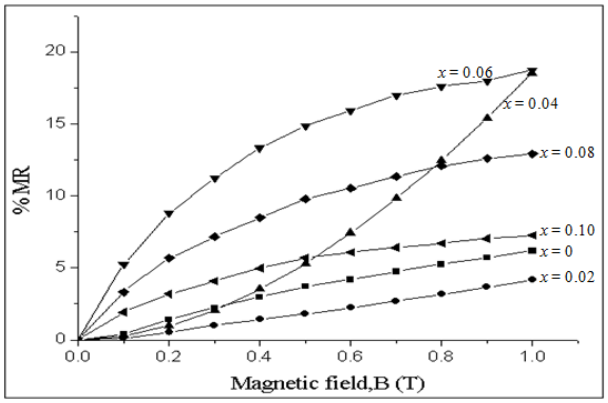

Figure 4 Magnetoresistance (%MR) versus magnetic field (B) of $La_{0.7}Ca_{0.3-x}Sr_xMnO_3$

Fig.5 shows graph of resistivity versus T^2 for $La_{0.7}Ca_{0.3-x}Sr_xMnO_3$ (x = 0, 0.02, 0.04, 0.06, 0.08, 0.10) series. From Table 3, ρ_o value decreases with increases of doping concentration except for x = 0.02 and x = 0.06. Jin et al. said that the ratio of Ca and Sr affects the resistivity which various as a function of T^2 in the thin films and the resistivity change appears to decrease with increase of x [17]. The quality of agreement between a theoretical equation and the experimental data of a material (best fit) can be tested by evaluating a statistical term, known as the square of linear correlation coefficient (R^2). It has been observed that R^2 found to be equal or greater than 0.98 for x = 0, 0.04, 0.06, and 0.10 (Table 3). In conclusion here, doping concentration of x = 0.02 and 0.08 does not fitted well to $\rho = \rho_o + \rho_2 T^2$.

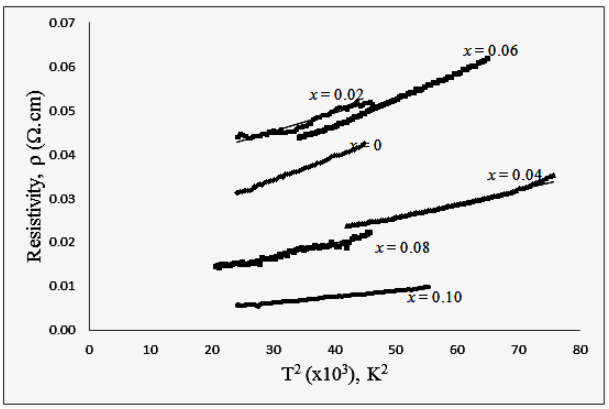

Figure 5 Resistivity versus temperature below T_{IM} of $La_{0.7}Ca_{0.3-x}Sr_xMnO_3$ with solid line fitted with $\rho = \rho_o + \rho_2 T^2$

Fig. 6 shows graph of resistivity versus $T^{2.5}$. The value of ρ_o, $\rho_{2.5}$, and R^2 for $La_{0.7}Ca_{0.3-x}Sr_xMnO_3$ (x = 0, 0.02, 0.04, 0.06, 0.08, 0.10) series that fitted to $\rho = \rho_o + \rho_{2.5}T^{2.5}$ are shown in Table 3. The ρ_o and $\rho_{2.5}$ values found to decrease with increasing strontium doping except for x = 0.06. It is interesting to note that the value of R^2 are found to be grater than 0.96 for all the samples except for x = 0.02 and may conclude that x = 0.02 is not fitted well to $\rho = \rho_o + \rho_{2.5}T^{2.5}$ for this research.

Table 3 ρ_2, ρ_o, R_2^2 (linear correlation coefficient), $\rho_{2.5}$, ρ_o, and $R_{2.5}^2$ of $La_{0.7}Ca_{0.3-x}Sr_xMnO_3$.

Sr doping	ρ_2 (ΩcmK^{-2})	ρ_o (Ω.cm)	R_2^2	$\rho_{2.5}$ (ΩcmK$^{-2.5}$)	ρ_o (Ω.cm)	$R_{2.5}^2$
x = 0	5.3 x 10^{-7}	0.0182	0.9978	2.9 x 10^{-8}	0.0210	0.9979
x = 0.02	4.1 x 10^{-7}	0.0330	0.9381	2.4 x 10^{-8}	0.0197	0.9442
x = 0.04	3.2 x 10^{-7}	0.0097	0.9852	1.4 x 10^{-8}	0.0152	0.9970
x = 0.06	5.9 x10^{-7}	0.0230	0.9981	3.2 x 10^{-8}	0.0288	0.9963
x = 0.08	3.0 x 10^{-7}	0.0037	0.9580	1.8 x 10^{-8}	0.0097	0.9607
x = 0.10	1.4 x 10^{-7}	0.0022	0.9914	8.0 x 10^{-9}	0.0032	0.9922

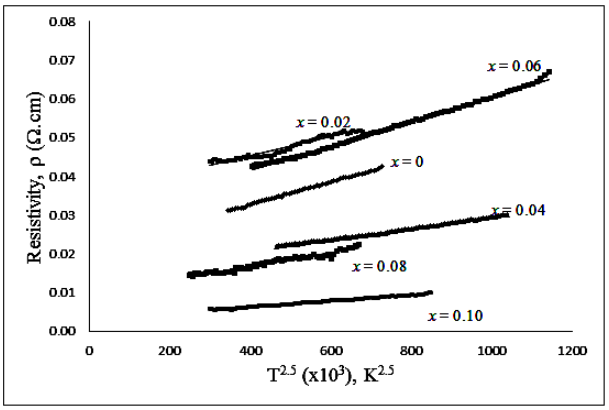

Figure 6 Resistivity versus temperature below T_{IM} of $La_{0.7}Ca_{0.3-x}Sr_xMnO_3$ with solid line fitted with $\rho = \rho_o + \rho_{2.5}T^{2.5}$

Fig. 7 shows the graph of ln $(\frac{\rho}{T})$ versus T^{-1}. The value of ρ_o and activation energy (E_a) was calculated from intercept of y-axis and slope of the graph. ρ_o values decrease with the increasing of doping concentration except for x = 0.06 while E_a values was found to increase with the increasing of doping concentration except for x = 0.06 (Table 4). Furthermore, it is also clear from Table 4, that the value of E_a for x = 0.06 are less compare to the remaining samples. This may be attributed to the oxygen deficiency. The oxygen deficiency induces an increase in the banding of Mn-O-Mn bond angle, thereby narrowing the bandwidth and enhancing the effective mass of the charge carrier. Due to this fact, the effective band gap increase with the increasing oxygen deficiency [27]. Activation energy is also due to the interface volume of grain size or grain boundary which is decreased in grain size and will increase grain boundary effect. But, in this research, the increase in grain size will increase the activation energy except for x = 0.06 which possesses the highest grain size value and the lowest activation energy (Table 2 and Table 4). It may due to the different of the grain sizes is not much (~ 0.2 µm) for x = 0 and x = 0.2.

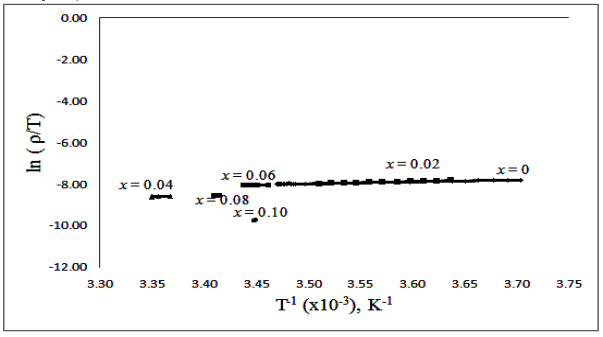

Figure 7 ln $(\frac{\rho}{T})$ versus T^{-1} with solid line fitted with $\rho_{SPH} = \rho_o \exp(\frac{E_a}{K_B T})$ of $La_{0.7}Ca_{0.3-x}Sr_xMnO_3$

Table 4 shows the value of R^2. It it seen that there is no trend for the value of R^2 when strontium doping concentration increases. It was indicated that the values of R^2 is larger than 0.92 for all the samples except for x = 0.10 which the values is 0.8795. Here, the conclusion is small polaron hoping model is not suitable for x =0.10 compared to the other sample.

Table 4 Pre-factor (ρ_o), activation energy (E_a), R^2 (the linear correlation coefficient), T_o and density of states at the Fermi level ($N(E_F)$ of $La_{0.7}Ca_{0.3-x}Sr_xMnO_3$.

Sr Doping	ρ_o (Ω cm K^{-1})	E_a (meV)	R^2	T_o (K)	$N(E_F)$ (eV^{-1}cm^{-3})	R^2
x = 0	3.0 x 10^{-4}	72.44	0.9946	1.2 x 10^6	1.5 x 10^{19}	0.9864
x = 0.02	2.7 x 10^{-4}	100.12	0.9954	6.7 x10^6	2.5 x 10^{18}	0.9958
x = 0.04	1.8 x 10^{-4}	108.77	0.9698	1.7 x 10^7	1.0 x 10^{19}	0.8042
x = 0.06	3.4 x 10^{-4}	35.58	0.9231	8.5 x 10^3	2.0 x 10^{21}	0.8348
x = 0.08	1.0 x 10^{-4}	452.55	0.9438	1.5 x 10^{10}	1.1 x 10^{15}	0.9835
x = 0.10	1.1 x 10^{-5}	2241.0	0.8795	4.6 x 10^{12}	3.7 x 10^{12}	0.8771

For variable range hoping model, graph ln ρ versus $T^{-0.25}$ were plotted (Fig. 8). The pre-factor (T_o) was increased with the increasing of strontium doping concentration except for x = 0.06 while $N(E_F)$ which decreases with the increasing doping concentration except for x = 0.06.

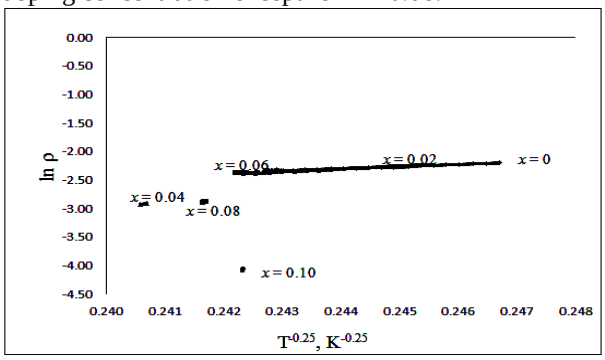

Figure 8 ln (ρ) versus $T^{-0.25}$ with solid line fitted with $\rho_{VRH} = \rho_o \exp\left(\frac{T_o}{T}\right)^{1/4}$ of $La_{0.7}Ca_{0.3-x}Sr_xMnO_3$

This observed behaviour can be explained on the basis of oxygen stoichiometry in the samples. The oxygen vacancies present in the material result in the reduction of Mn^{3+} (Mn^{4+}), thereby reducing double exchange mechanism between them, and as a result values of $N(E_F)$ decrease with increasing oxygen deficiency [27]. T_o values were inversely proportional to the grain size (Fig. 9). Table 4 shows that $N(E_F)$ increased with the decrease of T_o. Small polaron hoping model is more suitable to be used in these samples rather than variable range hoping model are know from the values of R^2 (the linear correlation coefficient).

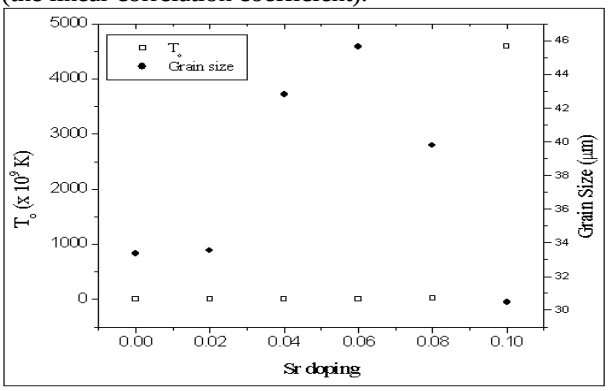

Figure 9 T_o and grain size dependence on the strontium doping concentration of $La_{0.7}Ca_{0.3-x}Sr_xMnO_3$

4. CONCLUSION

All samples are single phase with orthorhombic structure and *Pbnm* space group. There are no peak shifting and impurities observed when the doping concentration of strontium increases. T_{IM} values almost constant (~ 290 K) for x = 0.08 to x = 0.10. SEM micrograph shows that spiral-growth mechanism was observed for all the samples and x = 0.06 possesses the biggest grains size (~45.6 μm) compared to the others. The resistivity in the low temperature ferromagnetic metallic state may originate due to the electron-electron scattering process except for x = 0.02 and x = 0.08 and electron-magnon scattering process except for x = 0.02. In the high temperature paramagnetic insulating state, the resistivity may be explained by the small polaron hoping model and variable range hoping model for all the samples except for x = 0.06. Highest MR value are found when x = 0.06. Therefore, x = 0.06 can be choose as the best sample for sintering temperature of 1220°.

5. ACKNOWLEDGEMENTS

This work was supported by the Ministry of Science, Technology and Innovation, Malaysia (SciFund 03-02-03- SF 0217) and Ministry of Higher Education of Malaysia under Fundamental Research grant no. FRGS/FASA 1-2009/ SAINS TULEN/UNITEN/104 and UKM-DLP-2011-018.

6. REFERENCES

[1] Sunil Panwar, Vijay Kumar, Amit Chaudhary, Rajendra Kumar, Ishwar Singh. Theoretical study of magnetotransport properties of colossal magnetoresistive manganites (Re1-xAxMnO3): A variation treatment, Solid State Communication., pp223 (2015)

[2] G.H. Jonker and J.H. Van Santen,. Ferromagnetic compounds of manganese with perovskite structure. Physica 16(3): 337-349 (1950).

[3] G.H. Jonker, 1956. Physica 22, 707.

[4] A. Alexandrov, M. F. Mott. Polarons and Bipolarons, World Scientific, Singapore, (1995)

[5] H. Fehslee, H. Roder, G. Wellein, A. Mistriotis. Phys. Rev. B51, 16 582 (1995)

[6] C. Zener. Interaction between d shell in the transition metals, Phys. Rev. 81, 440 (1951).

[7] C. Zener. Interaction between d shell in the transition metal. II. Ferromagnetic compounds of manganese with perovskite structure, Phys. Rev. 82, 403 (1951)

[8] L.S. Ewe, R.Ramli, K.P.Lim, R.Abd-Syukor, Electrical and magnetotransport properties of magneto-resistive $La_{0.7}Ca_{0.28}Sr_{0.2}MnO_3$ prepared at different sintering temperature, Sains Malaysiana 41(6): 761-768 (2012.)

[9] Karmakar, S., Taran, S., Chaudhuri, B.K., Sakata, H., Sun, C.P., Huang, C.L. & Yang, H.D. Study of grain boundary contribution and enhancement of magnetoreisistance in La0 . 67Ca0.33MnO3 /V2 O5 composites. J. Phys. D: Appl. Phys. 38: 3757-3763 (2005)

[10] Ravi, V., Kulkarni, S.D., Samuel, V., Kale, S.N., Mona, J., Rajgopal, R., Daundkar, A., Lahoti, P. S. & Joshee, R. S. Synthesis of La0.7Sr0 . 3 MnO3 at 800o C using citrate gel method. Ceramics International 33: 1129-1132. (2007).

[11] Roul, B.K., Sahu, D.R., Mohanty, S. & Pradhan, A.K.. Effect of high temperature sintering schedule for enhanced CMR properties of La0.67Ca0.33MnO3 close to room temperature. Materials Chemistry and Physics 67: 267-271 (2001).

[12] Venkataiah, G., Prasad, V. & Venugopal Reddy, P. Influence of A-site cation mismatch on structural, magnetic and electrical properties of lanthanum manganites. Journal of Alloys and Compounds 429: 1-9 (2007).

[13] I.O. Troyanchuk, Sov,. Phys. JETP 75, 132 (1992).
[14] P. Shiffer et al,. Phys. Rev. Lett. 75, 3336 (1995).
[15] E. Dagotto, T.Hotta, A. Moreo,. Colossal Magnetoresistant Materials: the key role of phase separation, Phys. Rev. 344, 1-153 (2001).
[16] Shilpi Karmakar, S.Taran, B K Chaudhuri, H Sakata, C P Sun, C L Huang and H D Yang,. J. Phys. D:Appl. Phys. 38: 3757-3763 (2005).
[17] K. X. Jin, C. L. Chen, S. L. Wang, S. G. Zhao,Y. C. Wang, Z. M. Wang, Z. M. Song,. J. Materials Science and Eng, B119: 206 (2005).
[18] F. Moussa, M. Hennion, P. Kobu-Lehouelleur, D-Rezhik, S. Petit, H. Moudden, A-Ivanor, Va. M. Mukovskii, R.Privezentser, F. Albenque-Rullier,. Spin waves in the ferromagnetic metallic manganites $La_{1-x}(Ca_{1-y}S_y)_xMnO_3$, Phys. Rev. B76: 064403 (2007).
[19] Y. H. Jeong, S. H. Park, T. Y. Koo, K-B. Lee,.Solid State Ionic, 108: 249 (1998).
[20] H. S. Im, G. B. Chon, S. M. Lee, B. H. Koo, C. G. Lee, M. H. Jung, 2007. J. Magn. Magn. Material, 310: 2668-2670.
[21] L.S. Ewe, Imad Hamadneh, Hazar A. Salama, R. Abd-Shukor, 2008. Physica B 403: 2394-2398
[22] R. Mahendran, R. Mahesh, A. K. Raychaudhuri, C. N. R. Rao, 1996. Solid State Commu. 99, 3: 149
[23] P. Kameli, H. Salamati, A. Aezami, 2008. J. Alloys Compd. 450: 7.
[24] L.S. Ewe, I. Hamadneh, H. Salama, N.A. Nasri, S.A. Halim, R. Abd-Shukor, 2009. Appl Phys A, 95: 457-463.
[25] L. Sudheendra, H. D. Chinh, A. R. Raju, A. K. Raychaudhuri, C. N. R. Rao, 2002.Solid State Commun. 122: 53.
[26] Zhiqiang Jin, Wei Tang, Jianrong Zhang, Youwei Du, 1998. J. Magn. Mag. Mater. 187: 237-241.
[27] Y. Kalyana Lakshmi, G. Venkataiah, M. Vithal, P. Venugopal Reddy, 2008 Physica B 403: 3059